The Astrophysical Journal, 787:115 (10pp), 2014 June 1 doi:10.1088/0004-637X/787/2/115

AN EARLY LOOK OF COMET C/2013 A1 (SIDING SPRING): BREATHTAKER OR NIGHTMARE?

Quan-Zhi Ye (叶泉志)[1] and Man-To Hui (许文韬)[2]
[1] Department of Physics and Astronomy, The University of Western Ontario, London, Ontario N6A 3K7, Canada; qye22@uwo.ca
[2] Nhut Thung Pau Observatory, Guangzhou, China
Received 2014 March 10; accepted 2014 March 27; published 2014 May 9

ABSTRACT

The dynamically new comet, C/2013 A1 (Siding Spring), is to make a close approach to Mars on 2014 October 19 at 18:30 UT at a distance of 40 ± 1 Martian radii. Such an extremely rare event offers a precious opportunity for the spacecrafts on Mars to closely study a dynamically new comet itself as well as the planet–comet interaction. Meanwhile, the high-speed meteoroids released from C/Siding Spring also pose a threat to physically damage the spacecrafts. Here we present our observations and modeling results of C/Siding Spring to characterize the comet and assess the risk posed to the spacecrafts on Mars. We find that the optical tail of C/Siding Spring is dominated by larger particles at the time of the observation. Synchrone simulation suggests that the comet was already active in late 2012 when it was more than 7 AU from the Sun. By parameterizing the dust activity with a semi-analytic model, we find that the ejection speed of C/Siding Spring is comparable to comets such as the target of the *Rosetta* mission, 67P/Churyumov–Gerasimenko. Under a nominal situation, the simulated dust cone will miss the planet by about 20 Martian radii. At the extreme ends of uncertainties, the simulated dust cone will engulf Mars, but the meteoric influx at Mars is still comparable to the nominal sporadic influx, seemly indicating that an intense and enduring meteoroid bombardment due to C/Siding Spring is unlikely. Further simulation also suggests that gravitational disruption of the dust tail may be significant enough to be observable at Earth.

Key words: comets: individual (C/2013 A1) – meteorites, meteors, meteoroids – planets and satellites: individual (Mars)

Online-only material: color figures

1. INTRODUCTION

Near-Earth Objects (NEOs) play an important role in shaping the geological histories of terrestrial planets. Recent studies have shown that NEO impacts are common in the inner solar system (see, e.g., Strom et al. 2005). For other terrestrial planets, it has been suggested that the impact flux is comparable to the near-Earth environment (Le Feuvre & Wieczorek 2011). Although over 99% of the impactors are asteroids (Yeomans & Chamberlin 2013), comets are generally of special interest, as they carry a significant amount of volatile and organic material, which is essential for life. On Earth, kilometer-sized cometary impacts occur every $\sim 10^8$ yr (Stokes et al. 2003).

On the other hand, the close comet-planet approach is also significant in terms of the accretion of water and organic materials on the planet: comets eject a large amount of material into the vicinity of their nuclei, and they may still influence the planet without a direct impact. Although approaches are more common than impacts, they are still too rare for us to observe and study a real case: the closest cometary approach to the Earth since the establishment of modern science was D/1770 L1 (Lexell), which missed the Earth by ∼356 Earth radii. From the impact rates, we estimate that a close approach within 25 Earth radii with kilometer-sized comets occurs once every $\sim 10^5$ yr. This is equivalent to the frequency of cometary approach within 50 Martian radii to Mars assuming that the cometary impact flux (like the total impact flux) is comparable between Earth and Mars.

Yet this is what will happen later this year: a dynamically new (dynamically new) comet, C/2013 A1 (Siding Spring), is to miss Mars by ∼40 Martian radii on 2014 October 19.8 (UT) (Figures 1 and 2). C/Siding Spring was discovered on 2013 January 3 at a heliocentric distance of 7.2 AU; subsequent follow-up observations revealed a 10″ coma, which indicated distinct cometary activity at such a large heliocentric distance (McNaught et al. 2013). As of 2014 February 1, the comet is determined to be in a hyperbolic orbit, with $e = 1.0006$; C/Siding Spring is currently estimated to miss Mars by about 40 ± 1 Martian radii or 135,600 ± 6000 km.[3]

Dynamically new comets are constrained on loosely bounded or unbounded orbits, and are thought to originate from the outer region of the solar system, namely the Oort cloud. Due to the fact that they have had no access to the inner solar system, they preserve valuable and unique information about the pre-solar nebula. However, comparing with the periodical comets, which usually return to the inner solar system on a frequent and predictable basis, the dynamically new comets are difficult to investigate due to their small number and limited opportunity to study individual objects (generally only once). The most productive method to study comets—in-situ exploration—is currently very difficult to use on dynamically new comets, due to very short lead-times available for preparing and operating such missions.

As such, the close approach offers an unprecedented and extremely rare opportunity to directly study how material may be transferred from comets to terrestrial planets as well as the dynamically new comet itself. Currently there are three operational orbiters (the *Mars Reconnaissance Orbiter*, *Mars Odyssey*, and *Mars Express*) and two operational rovers (Opportunity and Curiosity) on Mars; in addition, two orbiters (the *Mars Atmosphere and Volatile Evolution* or *MAVEN*, and the *Mars Orbiter Mission* or *MOM*) will arrive ∼1 month before C/Siding Spring's closest approach. The fleet will have front row seats for this

[3] Update numbers can be found at http://ssd.jpl.nasa.gov/sbdb.cgi?sstr=2013A1.

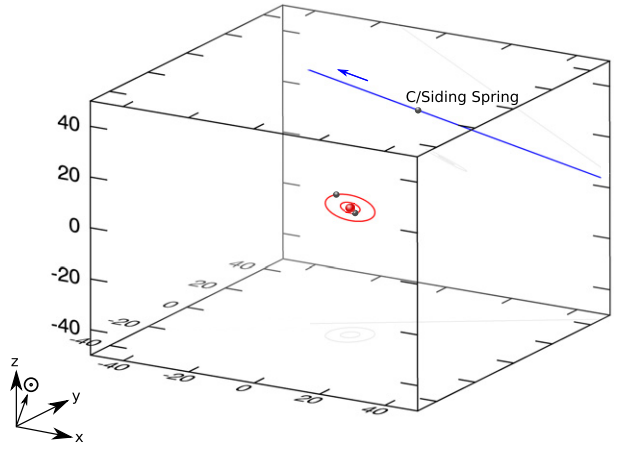

Figure 1. Close approach of C/Siding Spring to Mars. The plot is constructed in J2000 ecliptic frame where 1 unit equals 1 Martian radii. The two objects orbiting Mars (center object in red) are the two Martian moons, Phobos (inner) and Deimos (outer). The sizes of the objects are not to scale.

(A color version of this figure is available in the online journal.)

event; however, the small distance by which the comet will miss the planet also means that they may pass inside the dust coma/tail of C/Siding Spring. While the Martian atmosphere will shield incoming dust particles (meteoroids) for the two rovers, the five orbiters will be at risk for the bombardment of dust particles originating from the comet. Cometary dust poses a significant threat of causing physical damage to the spacecrafts (see, e.g., A'Hearn et al. 2008). Additionally, meteoroids originating from C/Siding Spring have higher kinetic energy than nominal sporadic (background) meteoroids, as the relative speed of the comet is twice as high as that of Mars. Early studies of C/Siding Spring before its close visit to Mars will be essential to monitor the evolution of the comet and help assess the risk posed to the spacecrafts.

Here we present our observations and modeling effort of C/Siding Spring in the hope of characterizing the physical properties of the comet. We will first discuss our observations and their significance for constraining the particle size distribution (PSD) of the comet. Then we will present the semi-analytic model that will be used to match the observation and parameterize the cometary dust activity. Eventually, we will use the best-matched parameters to investigate the fluency of cometary dust particles experienced by Mars (and anything in the proximity) during the close encounter.

2. OBSERVATIONS AND INITIAL INTERPRETATION

2.1. Planning and Conducting the Observations

After being released by the parent body, different sizes of dust particles follow different Keplerian trajectories due to different amounts of radiation pressure and gravity from the Sun. The ratio of the later two quantities is defined as β, of which $\beta \propto (\rho r)^{-1}$, where ρ is the particle density and r is the size. If we ignore the initial velocity of the particles with respect to the nucleus and compute a large number of particles with different β released at different times, we can produce the so-called syndyne–synchrone diagram as defined by Finson & Probstein (1968).

Occasionally, the Earth–comet geometry is favorable to so that different syndyne curves (i.e., equal-β curves) are well separated from each other as seen by the observer, which allows us to qualitatively constrain the PSD of the comet. The occurrence of such geometry depends on the orientation of the orbital plane of the comet. We discover that for C/Siding Spring, such geometry would have occured in 2013 September to November, while the solar elongation of the comet is adequate for optical observations (Figures 3 and 4). The next "slots" will occur in 2014 June and September, but they either suffer from small solar elongation or from being too close to the encounter event.

We conduct broadband observations with a 0.18 m $f/7$ refraction telescope and 4k × 3k CCD camera (pixel size 1.″5) at the Jade Scope Observatory near Siding Spring, Australia (149°12′ E, 31°17′ S), on 2013 November 12, 20, and 23 (details summarized in Table 1). Observations are unfiltered and the CCD sensor is most sensitive at ∼500 nm. The raw frames

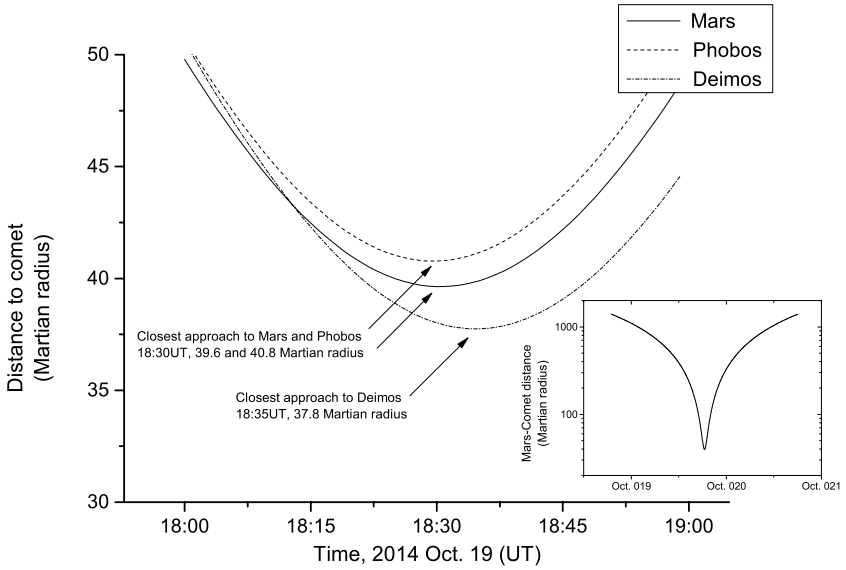

Figure 2. Distance between C/Siding Spring and Mars, Phobos, and Deimos within 30 minutes of the closest approach (the inset shows the Mars–comet distance within 1 day of the closest approach). The miss distances have an uncertainty of ∼1 Martian radius.

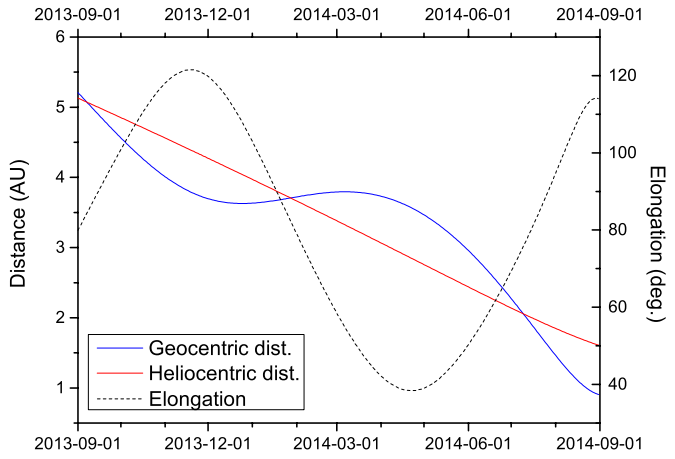

Figure 3. Observation circumstances of C/Siding Spring from 2013 September to 2014 August.

(A color version of this figure is available in the online journal.)

are then subtracted by dark and bias fields and divided by flat fields. After the initial reduction, the frames are registered with the NOMAD catalog (Zacharias et al. 2004) so that they can be combined and stacked following the motion of C/Siding Spring. Eventually, we end up with three "master" images from each night (Figure 5).

2.2. Is C/Siding Spring Rich in Big Particles?

We compute the syndyne–synchrone curves for the three master frames (Figure 6) and immediately notice that C/Siding Spring's tail is skewed to smaller β values (i.e., larger particles), dominantly of the order of 0.01. If we use $\beta = 5.74 \times 10^{-4}/(\rho r)$ (Williams & Fox 1983) and assume $\rho = 300$ kg m^{-3}, $\beta = 0.01$ is equivalent to $r = 200\,\mu$m or 10^{-9} kg for a spherical particle. This number is significant because 10^{-9} kg is considered to be the lower end of the threat regime by spacecraft designers (McNamara et al. 2004). Since optical observation strongly favors micron-sized particles due to their higher scattering efficiency, the absence of a tail structure at larger β suggests that the cometary tail is dominated by larger, spacecraft-threatening particles.

Table 1
Observation Circumstances of the C/Siding Spring Data

Date (UT)	Exposure	Total Frames	Airmass	r_h (AU)	Δ (AU)
2013 Nov 12.63	90 s	34	1.010	4.450	3.857
2013 Nov 20.56	90 s	60	1.019	4.374	3.776
2013 Nov 23.59	90 s	63	1.012	4.345	3.750

3. THE DUST TAIL MODEL

3.1. Philosophy of the Model

We develop a semi-analytic dust tail model (DTM) to parameterize the cometary dust tail. The key of parameterization involves the initial velocity, i.e., the velocity vector of the particles at the time of its ejection from the cometary nucleus. We start from the revised Whipple's (1951) model by Brown

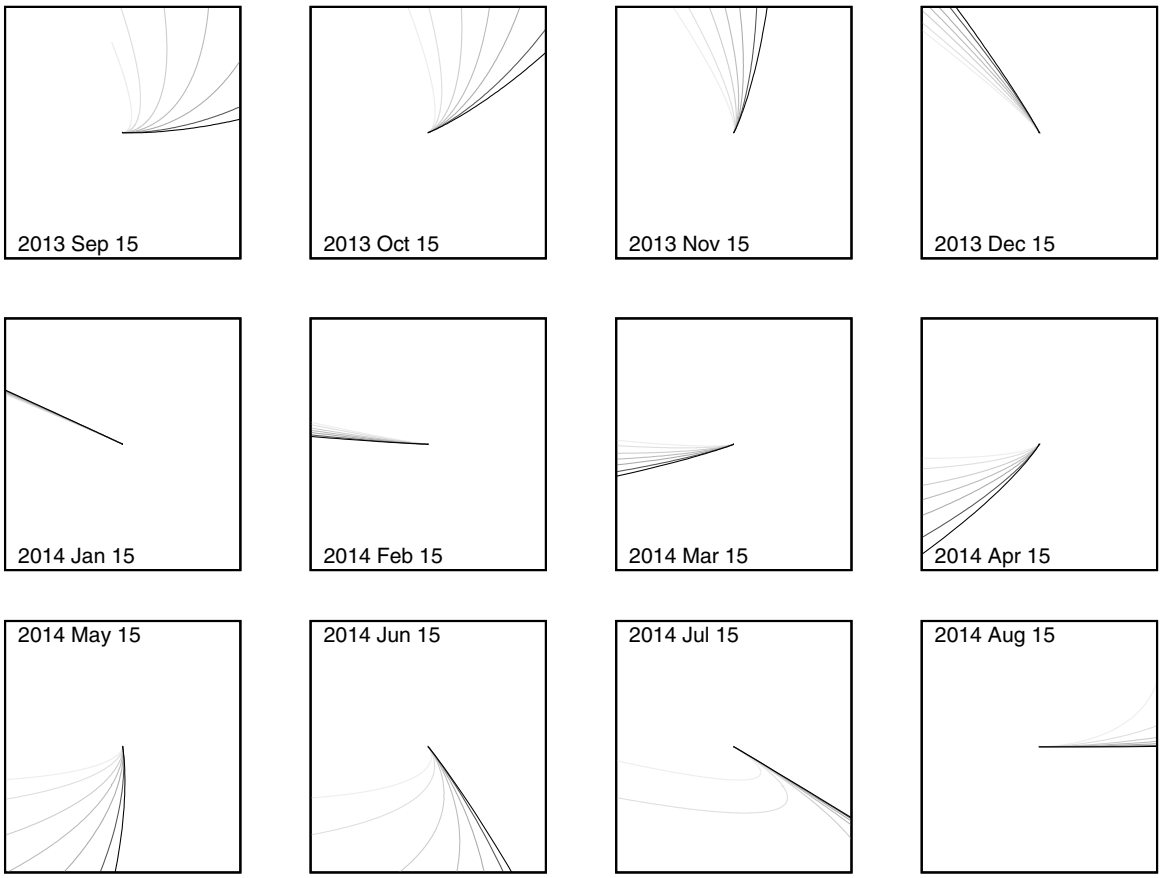

Figure 4. Syndyne simulations of C/Siding Spring from 2013 September to 2014 August. β ranges from 0.01 (light gray) to 1 (black). Each diagram is $10' \times 10'$ in size, north is up and east is left.

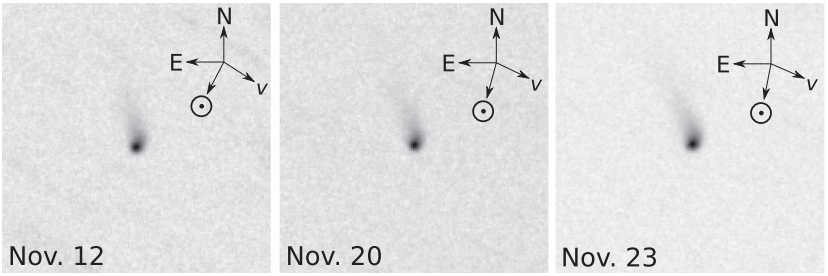

Figure 5. Master frames of the observations on 2013 November 12, 20, and 23. Each image is $6' \times 4'$.

& Jones (1998), which was used to study the Perseid meteor stream formed by 109P/Swift–Tuttle:

$$V = (10.2\ \mathrm{m\ s^{-1}}) \left(\frac{r_h}{1\ \mathrm{AU}}\right)^{-\frac{1}{2}} \left(\frac{\rho}{1\ \mathrm{g\ cm^3}}\right)^{-\frac{1}{3}} \times \left(\frac{r_C}{1\ \mathrm{km}}\right)^{\frac{1}{2}} \left(\frac{m}{1\ \mathrm{g}}\right)^{-\frac{1}{6}}, \quad (1)$$

where V is the ejection velocity relative to the nucleus in m s^{-1}, r_h is heliocentric distance of the comet, ρ is the bulk density of the meteoroids, r_C is the radius of the cometary nucleus, and m is the mass of the meteoroid.

Brown & Jones reported a satisfactory agreement between the model and the observation for the case of the Perseid meteor stream; however, they noted that the agreement might be due to the nature of the high-ejection velocity of P/Swift–Tuttle and that it may not be applicable to other comets. To accommodate this issue, we introduce a "reference" ejection velocity which has been used in other studies (e.g., Ishiguro et al. 2007) and rearrange the terms:

$$V = V_0 \left(\frac{r_h}{1\ \mathrm{AU}}\right)^{-u} \left(\frac{a}{a_0}\right)^{-\frac{1}{2}} \left(\frac{\rho}{\rho_0}\right)^{-\frac{1}{2}} \left(\frac{d_C}{1\ \mathrm{km}}\right)^{\frac{1}{2}}, \quad (2)$$

where V_0 (in m s^{-1}) is a reference ejection velocity of particles with size of $a_0 = 5$ mm and a bulk density of $\rho_0 = 1000$ kg m^{-3} ejected by a cometary body of a diameter of 1 km at a heliocentric distance of 1 AU, and u is the dependence on the heliocentric distance; the introduction of u will be elaborated upon in the next section. The V_0 corresponding to the constant of 10.2 in Brown & Jones' model would be $V_0 = 8.0$ m s^{-1}. We assume that the particles are symmetrically released at the comet's sub-solar point at a direction of $w < 45^\circ$ from the sunward direction. This w limit is chosen following the results of Ishiguro et al. (2007) and Ishiguro (2008).

The initial velocity model is fed by a Monto–Carlo subroutine that generates random particle with sizes following a power law: $N(a) = (a/a_0)^q$, where $N(a)$ is the accumulative particle number, and q is the size distribution index. We then solve Kepler's equation rigorously from the start time to the time of the observation to determine the position of the particle. These steps are repeated until we have a sufficient number of particles to simulate the morphology of the cometary tail.

At the end, we compute the spatial intensity on a sky plane coordinate (α, δ). We consider a simple model without secondary effects such as the response efficiency of the CCD sensor to different wavelength and the scattering efficiency due to particle shape. We consider the light contribution from each particle:

$$I'(a, r_h) = \left(\frac{r_h}{1\ \mathrm{AU}}\right)^{-2} a^2 A_p, \quad (3)$$

where A_p is the modified geometric albedo. The intensity at (α, δ) will just be the sum of intensities from all particles within the region ($d\alpha' d\delta'$):

$$I(\alpha, \delta) = \int\int I'(a, r_h) d\alpha' d\delta'. \quad (4)$$

Finally, a two-dimensional intensity map is created by looping around all possible (α, δ) and computing the value of $I(\alpha, \delta)$ at each position.

Table 2
Observation Circumstances of the C/ISON Data

Date (UT)	Instrument	Pixel Size (pixel^{-1})	Exposure	Total Frames	r_h (AU)	Δ (AU)
2012 Oct 17.90	0.35 m SASP	0.″9	90 s	50	6.029	6.051
2013 Feb 2.69	0.35 m SASP	0.″9	90 s	60	4.916	4.026
2013 May 15.64	0.35 m SASP	0.″9	60 s	34	3.710	4.342
2013 Aug 31.92	0.11 m XP1	3.″5	60 s	10	2.179	2.973
2013 Sep 26.91	0.11 m CSP	3.″5	120 s	30	1.726	2.667
2013 Oct 26.94	0.35 m SASP	0.″9	20 s	20	1.116	1.374

3.2. Determining the u Constant

The treatment of u is somewhat tricky, as a number of u values have been suggested by previous workers. For example, some studies from both cometary and meteor communities suggested $u = 0.5$ (e.g., Crifo 1995; Brown & Jones 1998; Ishiguro et al. 2007; Ishiguro 2008), Whipple's (1951) original model suggested $u = 1.125$, while $u = 1$ (Brown & Jones 1998; Reach et al. 2000; Ma et al. 2002) and $u = 3$ (Agarwal et al. 2010) were also used. We note that most studies that adopted $u = 0.5$ do not have data that cover a broad range of r_h; our initial test with $u = 0.5$ also shows a noticeable mismatch at large r_h (e.g., $r_h > 3$ AU). This may be due to the fact that the range of r_h is not broad enough to constrain u more effectively, but could also be due to, for example, the onset of water–ice sublimation at ~2.3 AU which dramatically enhances the ejection regime and hence no unique u can be defined.

To investigate this matter, we use the observations of C/2012 S1 (ISON), which are available for a broad range of r_h. The unfiltered observations were taken at the Xingming Observatory, China, from a few days after the discovery ($r_h = 6.2$ AU) to a few weeks before the perihelion ($r_h \lesssim 1$ AU; see Table 2). The DTM model is run at grids with $u \in [0.5, 4.0]$ and $V_0 \in [1.0, 8.4]$ m s^{-1}, with orbital elements from JPL 54 (Table 3). A few parameters at the far ends are not tested as initial trials indicate that they are unlikely to contain the best fits.

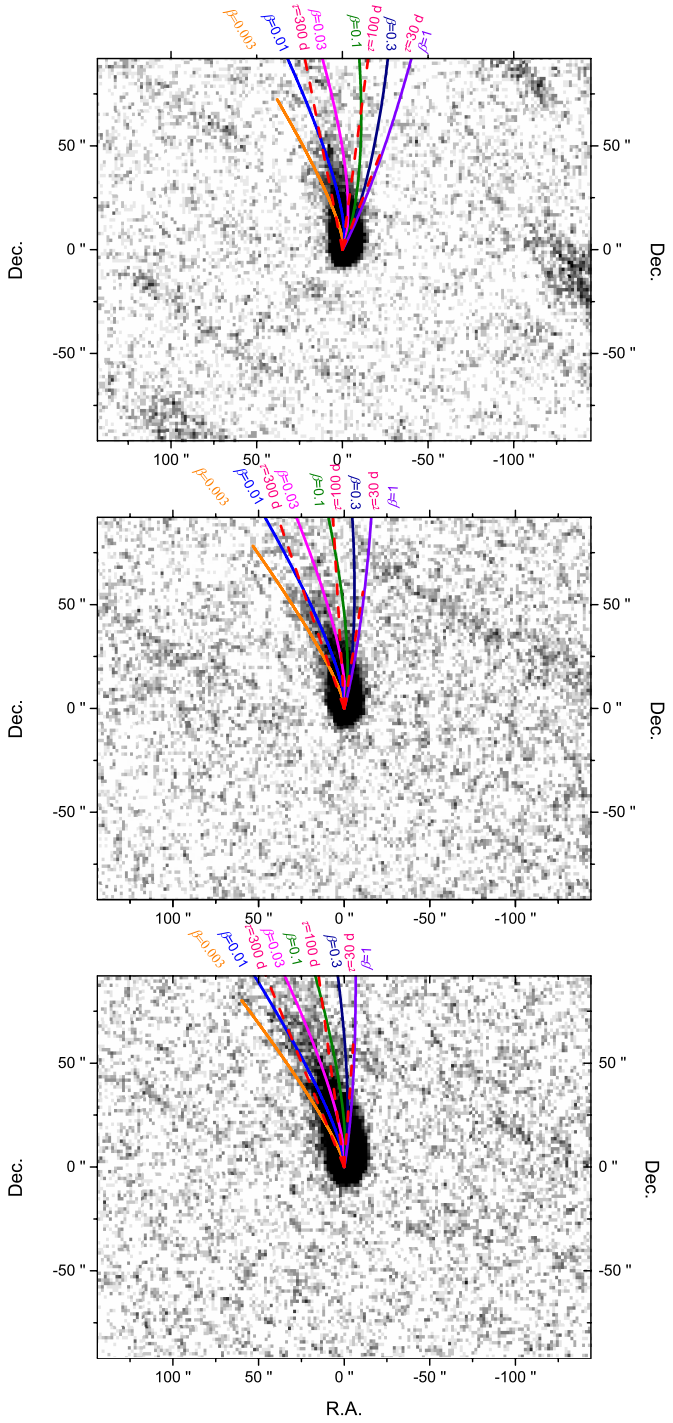

Figure 6. Syndyne–synchrone computation for the master frames. North is up and east is left.

(A color version of this figure is available in the online journal.)

Except for the nucleus size of C/ISON, which has been reported to be of the order of 1 km (Knight & Walsh 2013; Li et al. 2013), we must make some assumptions, such as the albedo and particle density. Although the nucleus size will not effectively affect our final result (since its contribution is modest in most cases and can be balanced by a slightly larger or smaller V_0 term), we still keep it in the simulation as we hope that V_0 can be comparable to C/Siding Spring and other comets. The set of parameters are summarized in Table 4. The simulation results and the observations are then compared and graded separately by both authors on a Boolean basis (i.e., as "possible fit" or "definitely not a possible fit"). Finally, the grades are summed and it is rated on a scale from 0 to 100.

Table 3
Orbital Elements (in J2000) of C/ISON (from JPL 54) and C/Siding Spring (from JPL 40) Used for the Simulation

Element	C/ISON	C/Siding Spring
q (AU)	0.01245259	1.3991521
e	1.000201	1.00057866
i	62.°4039775	129.°025859
Ω	295.°6520316	300.°972350
ω	345.°5312406	2.°432872
t_p (UT)	2013 Nov 28.77866	2014 Oct 25.40490

Table 4
DTM Parameters for the Simulation of C/ISON

Parameter	Symbol	Value
Maximum τ (days)	$\tau_{\max}$	365
Particle size (m)	a	$[10^{-5}, 10^{-2}]$
Size distribution index	s	−2.6
Modified geometric albedo	A_p	0.04
Number-distance constant	k	−3.0
Bulk density of particle (kg m^{-3})	ρ	300
Size of cometary nucleus (km)	d_C	1
Dependence constant on heliocentric distance	u	0.5, 1.0, 1.5, 2.0, 3.0, 4.0

Table 5
DTM Parameters for the Simulation of C/Siding Spring

Parameter	Symbol	Value
Maximum τ (days)	$\tau_{\max}$	1000
Particle size (m)	a	$[10^{-4}, 10^{-2}]$
Size distribution index	s	−2.6
Modified geometric albedo	A_p	0.04
Number-distance constant	k	−3.0
Bulk density of particle (kg m^{-3})	ρ	300
Size of cometary nucleus (km)	d_C	5
Dependence constant on heliocentric distance	u	1.0

The final score chart (Figure 7) indicates that with $V_0 = 2.1$ (m s^{-1}), $u = 1.0$ is the best fit. It is encouraging that no dramatic morphological change is presented near the water–ice sublimation line (~2.3 AU), which means that the u we found is a unique approximation to the entire r_h range. The change in the $r_h = 1.1$ AU case is most likely due to the contamination from cometary gas emission, as no filters were used to block the primary emission lines (e.g., C_2 and C_3 which falls in the $\lambda = 500$ nm range where the imaging CCD is sensitive); we may remove the $r_h = 1.1$ AU case and it does not alter our result.

3.3. Simulation Result

After pinned down the u constant, we run the DTM model for the case of C/Siding Spring with V_0 ranging from 1.0 to 4.2 m s^{-1} to determine V_0. The input parameters and orbital elements are summarized in Tables 3 and 5. Since the epochs of our observations are fairy close, we only simulate the November 23 case, as the master frames were stacked from more frames and had a slightly better airmass. We estimate $d_C = 5$ km considering two comparable comets in which the nucleus diameters are constrained at a higher level of confidence: 19P/Borrelly (M1 = 8.9, M2 = 13.8, $d_C = 4.8$ km)[4] and

[4] http://ssd.jpl.nasa.gov/sbdb.cgi?sstr=19P, retrieved 2014 March 2.

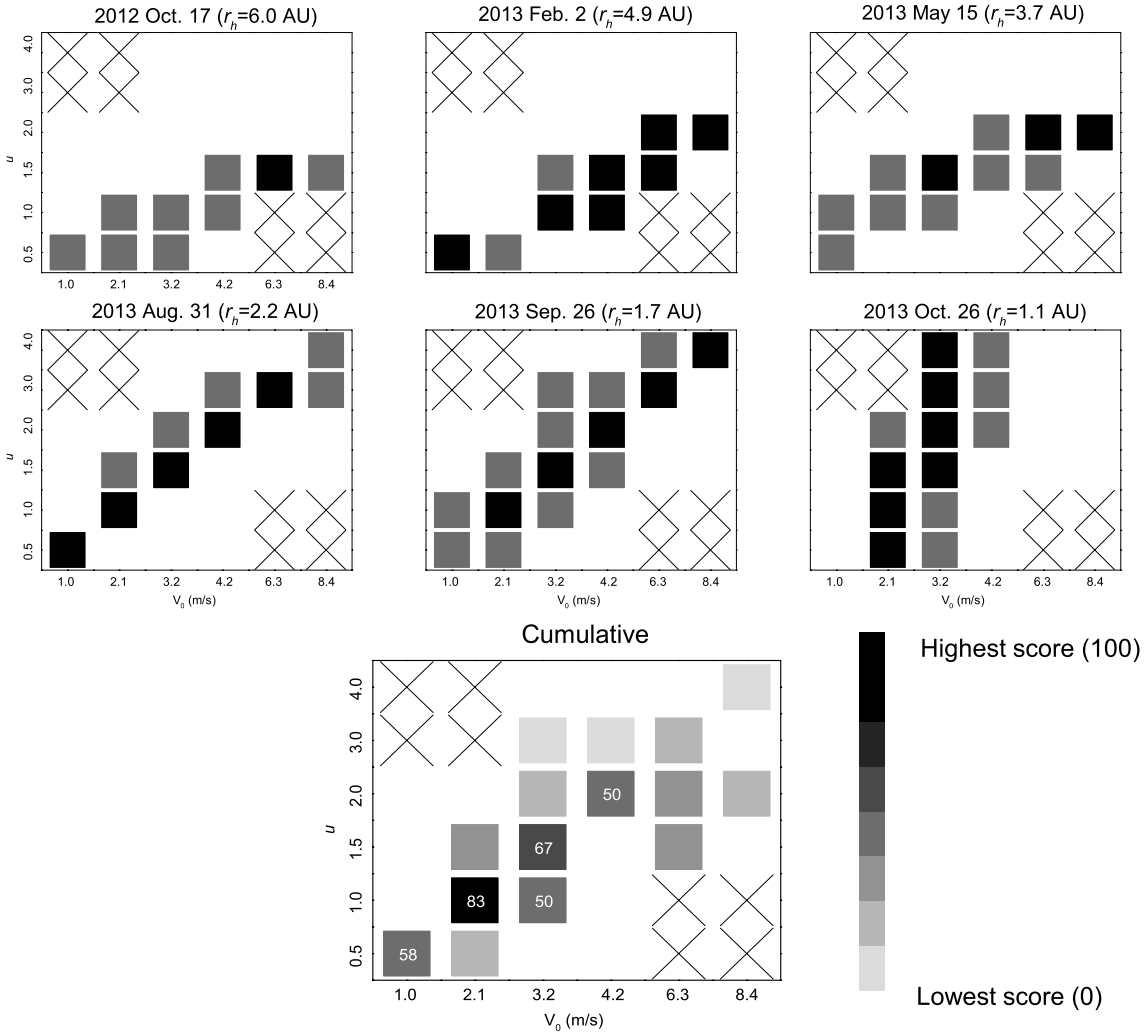

Figure 7. Score charts for C/ISON for determining the u constant. Crosses indicate the trials that are not evaluated. Scores (between 0 and 100, with 100 being the highest) are listed if >50.

C/1996 B2 (Hyakutake) (M1 = 7.3, M2 = 11.1, d_C = 4.2 km),[5] in contrast, C/Siding Spring has M1 = 8.6, M2 = 10.4.

The simulation result is shown in Figure 8. Comparing the simulation to the observation (Figure 5), we see V_0 = 1.0 m s^{-1} as the optimal match. We note that the strong size gradient indicated in the syndyne diagram (Figure 6) actually forged the result: since optical observation strongly favors smaller particles that dominate the west-end sector of the tail (i.e., toward the clockwise direction), the west-end boundary (about P.A. $\sim$ 345°) marks the true boundary of the tail. As we only simulate particles with $\beta < 0.01$, the simulated particles should mostly be distributed within the anticlockwise direction of P.A. $\sim$ 345°, which is only satisfied by the V_0 = 1.0 m s^{-1} case. Such converge allows us to make a stronger conclusion on the optimal V_0.

The V_0 = 1.0 m s^{-1} value is comparable to some comets that were previously studied, including 4P/Faye, 22P/Kopff, and the *Rosetta* mission target, 67P/Churyumov–Gerasimenko (see, e.g., Ryabova 2013; note that the V_0 value here needs to be ×4 to make the numbers comparable), although the dynamical origins of these comets seem to be different. It is interesting to note that this similarity comes with the fact that comets with similar dynamical origins can great deviations in V_0: for example, V_0 for 2P/Encke is about a magnitude larger. This may be purely by coincidence, but further studies with larger sample sizes may determine if there are any physical causes.

4. ENCOUNTER

Eventually, we run the simulation for the encounter with best-fit parameters found in the previous iterations (summarized in Table 5) to study the influence of cometary dust on Mars and its vicinity. Unlike other meteor stream models, our model does not include planetary perturbation; however, we believe that this is acceptable for the case of C/Siding Spring since the comet is far from the ecliptic plane (i = 129°) until the encounter.

The synchronic feature in Figure 6 suggests that C/Siding Spring was active at least a year before our observations; therefore we choose $\tau_{\max}$ = 1000 days (corresponding to 2012 January 23) as the start date of the simulated cometary activity to catch any early activities. State vectors of simulated particles are recorded within ±1 day of the closest encounter (2014 October 18, 18:30 UT to 2014 October 20, 18:30 UT) in a time-step of 1 minute. Since simulating the entire set of cometary particles will take quite a bit of time (comets typically release particles at a rate of $\sim 10^7$–10^{10} s^{-1}), we only simulate a representative number of particles and scale them up afterward.

[5] http://ssd.jpl.nasa.gov/sbdb.cgi?sstr=1996+B2, retrieved 2014 March 2.

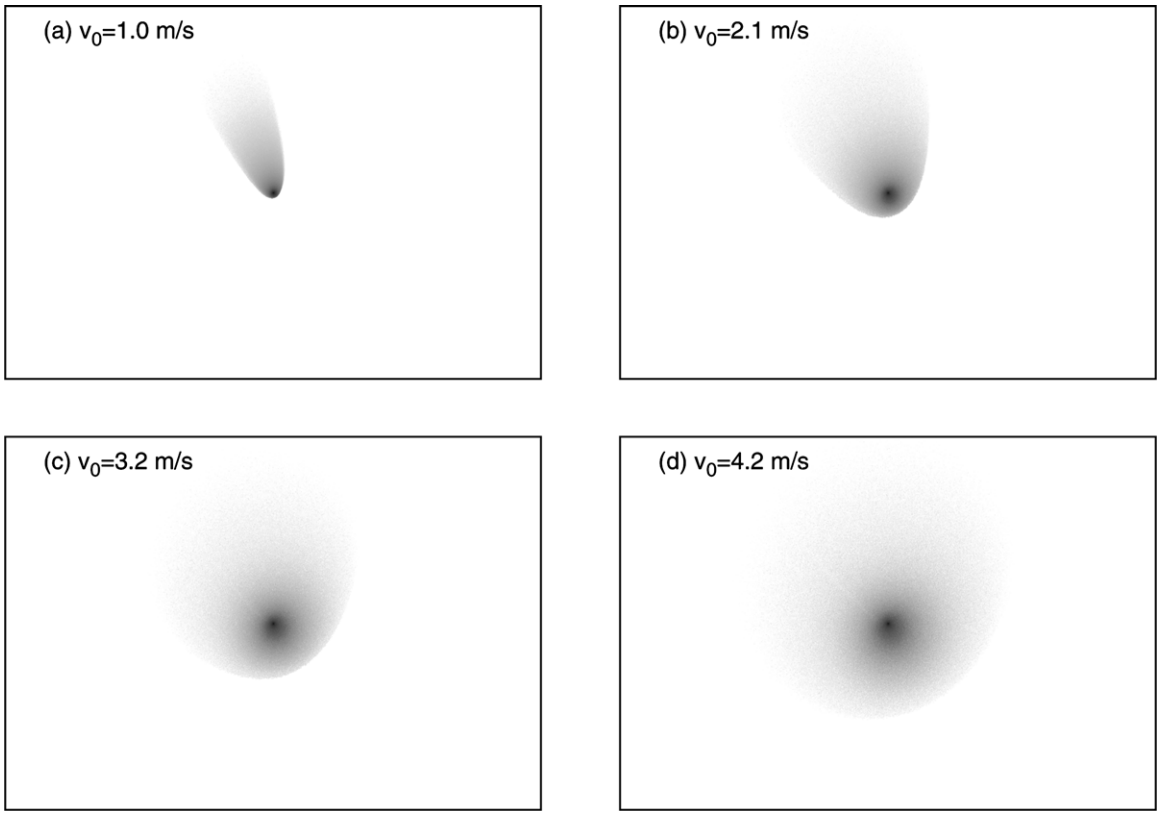

Figure 8. DTM simulation for the master frame of C/Siding Spring on 2013 November 23. The size of each figure is $8' \times 4'$. North is up and east is left.

We first need to examine the dust production rate of C/Siding Spring; this can be tied to the so-called $Af\rho$ quantity (A'Hearn et al. 1984). The number of ejected particles in the particle size range (a_1, a_2) can be related to $Af\rho$ by (Vaubaillon et al. 2005; Ye & Wiegert 2014)

$$Q_g(a_1, a_2) = \frac{655 A_1(a_1, a_2) Af\rho}{8\pi A_B j(\phi)[A_3(a_1, a_2) + 1000 A_{3.5}(a_1, a_2)]}, \quad (5)$$

where $A_x = (a_2^{x-s} - a_1^{x-s})/(x-s)$ for $x \neq s$ and $A_x = \ln(a_2/a_1)$ for $x = s$, where s is the size population index, A_B is the Bond albedo, and $j(\phi)$ is the normalized phase function.

We obtain the $Af\rho$ measurements conducted by a group of observers and collected by the "Cometas Obs."[6] The measurements show a steady $Af\rho$ near 1500 cm from $r_h = 6.76$ AU to $r_h = 3.72$ AU. By assuming $Af\rho \propto (q/r_h)^{4/3}$ when the comet gets into the water–ice sublimation line (to include possible early onsets, we use a loose constraint, $r_h \simeq 3$ AU), we estimate the $Af\rho$ of C/Siding Spring at 1 AU to be 3700 cm, which corresponds to $N_0 = 3 \times 10^{10}$ s^{-1}.

The result is shown in Figure 9: Mars will miss the dust cone by some 20 Martian radii or 67,800 km.

What about the extreme cases in the uncertainty ranges? To investigate this, we run further simulations with some educated guesses about the uncertainty ranges: a factor of 10 for the minimum particle size, a factor of 2 for the diameter of the cometary nucleus, and 50% for the reference velocity. Four combinations are tested while the other parameters remain the same as in Table 5. The combinations and results are shown in in Table 6 and Figure 10.

[6] Available at http://www.astrosurf.com/cometas-obs/C2013A1/afrho.htm, retrieved on 2014 February 6.

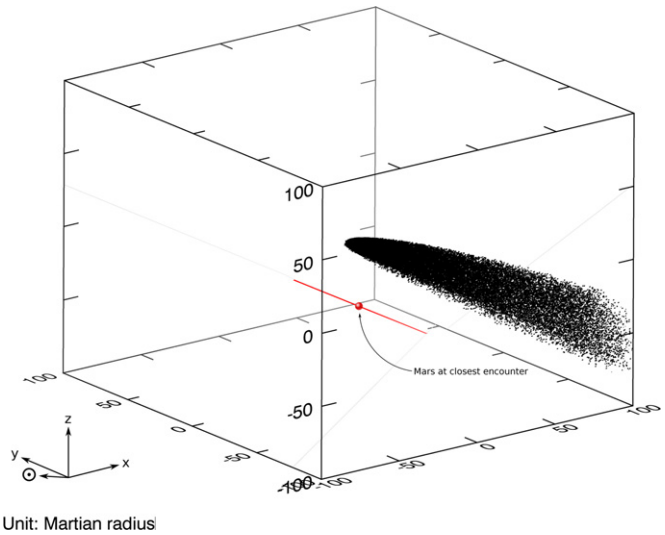

Figure 9. DTM simulation result together with the trajectory of Mars shown in a cometocentric ecliptic frame.
(A color version of this figure is available in the online journal.)

For scenario 4, in which the minimum particle size/mass remains unchanged (i.e., particles are confined to within the spacecraft-threatening category), we still find no direct encounter between Mars and the dust cone. For the other three scenarios, the dust cone does reach Mars. The peak times are about 30–60 minutes behind the closest approach. We see some "peak-lets" in the time series plots which should be artifacts due to low statistics rather than any physical explanations. The low statistics also make it difficult to determine the duration of the event, but we can crudely estimate the FWHM to be ~1 hr or

Table 6
The Meteoroid Influence at Mars under Four Extreme Cases in the Uncertainty Ranges

Scenario	1	2	3	4
Condition	$a_{\min} \times 0.1$	$a_{\min} \times 0.1$ $d_C \times 2$	$a_{\min} \times 0.1$ $d_C \times 2$ $V_0 \times 1.5$	$d_C \times 2$ $V_0 \times 1.5$
Active time (approx.) (UT, 2014 Oct 19)	19:20–20:45	18:30–20:55	18:05–21:50	N/A
Peak time and flux (UT, 2014 Oct 19)	19:27	19:26	18:51	N/A
Peak flux (m^{-2} s^{-1})	1.3×10^{-7}	1.3×10^{-7}	4.7×10^{-7}	N/A
FWHM	<1 hr	<1 hr	1 hr	N/A
Total flux (m^{-2})	2.6×10^{-6}	4.8×10^{-6}	1.8×10^{-5}	N/A

less. The peak fluxes are on the order of 10^{-7} m^{-2} s^{-1} while the accumulative fluxes are on the order of 10^{-5} m^{-2}, appropriate for the meteoroids larger than 10^{-12} kg. The absence of an encounter in scenario 4 suggests that the particles that arrive at Mars in scenarios 1–3 are in the range of 10^{-12} to 10^{-9} kg, which are below the spacecraft-threatening regime.

5. DISCUSSION

5.1. Comparison with Moorhead et al. (2014)

Moorhead et al. (2014) also studied the meteoroid influence on Mars during the encounter of C/Siding Spring but with a different approach: they construct a symmetric analytic model of the coma that relates the dust production rate to the total magnitude (M1) of the comet. As a separate check, the meteoroid flux experienced by Giotto and Stardust spacecrafts during their encounter with 1P/Halley and 81P/Wild were reproduced by this model and compared with the actual data, and order-of-magnitude agreements were found. Since more parameters were unconstrained at the time of their study, they parameterized their result and reported an accumulative flux of 0.15 m^{-2} for particles over 4.19×10^{-9} kg under nominal conditions. They also conducted simulation with a dynamical meteor stream model that uses Brown & Jones's (1998) ejection model (P. A. Wiegert 2013, private communication) and found that the numbers from the two models agreed within an order of magnitude, although the number from the dynamic model is in fact lower by a factor of two, which they attributed to the difference in modeling assumptions.

Since their study, the M1 of C/Siding Spring has been revised from 5.2 to 8.6; using Equation (18) in their study and $\rho = 300$ kg m^{-3}, we find a new value of 0.0135 m^{-2}. This is still more than three orders of magnitude higher than our result. To investigate this difference, we test our model with V_0 set to the value equivalent to the Brown & Jones's (1998) model and find a much closer value ($\sim$0.001 m^{-2}), which would allow an order-of-magnitude agreement to Moorhead et al.'s result from the dynamical model. From here we suggest that the difference between the two results is primarily caused by different input parameters.

5.2. Implications for the Spacecrafts, Rovers, and Martian Moons

The sporadic meteoroid influx on Mars is about half of the influx on Earth (Domokos et al. 2007) or $\sim 1.8 \times 10^{-8}$ m^{-2} s^{-1} for a meteoroid larger than 10^{-9} kg. For comparison, the peak flux of the 2012 Draconid meteor storm is 3.3×10^{-6} m^{-2} s^{-1} for a meteoroid larger than 10^{-9} kg, assuming a general power law distribution (Ye et al. 2014).[7] From here, our simulation seems to indicate that the meteoric influx on Mars due to C/Siding Spring is comparable to the sporadic background. For the case of smaller-sized meteoroids, the sporadic influx is about 3 mag higher from 10^{-9} kg to 10^{-12} kg, which would still put the influx due to C/Siding Spring no higher than the sporadic background. The simulation also suggested that the bulk of the outburst (if any) would not be longer than the orbital period of the orbiters around Mars. For the Opportunity and Curiosity rovers, the potential meteor outburst takes place during the Martian morning and afternoon, respectively, which prevents any meteor observations from reaching the rover.

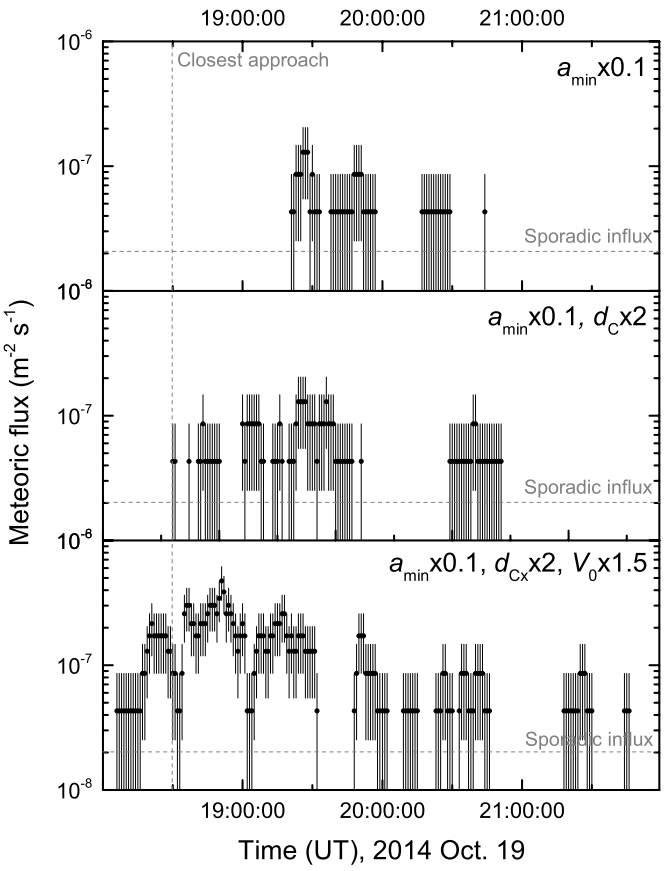

Figure 10. Meteoroid influx at Mars in three scenarios (see the main text). The uncertainty bar depicts the Poisson error ($\sigma = \sqrt{N}$). The "peak-lets" of fluxes are due to low statistics.

The impact on the Martian moons is another interesting topic. At the time of the encounter, Deimos will be about 2 Martian radii closer to the cometary nucleus than Mars itself. Depending on its physical properties and impact angle, a 200 μm meteoroid may produce a sub-meter crater on Phobos and Deimos.[8] Unfortunately, such a crater is below the resolution of our current best images (about 5 m $pixel^{-1}$), but it is worth pointing out that the high-speed nature of meteoroids originating from C/Siding Spring should create larger craters more efficiently than nominal sporadic meteoroids.

[7] The power law distribution is quoted from Ceplecha et al. (1998, Table XXVI), which suggested a factor of $10^{3.69}$ between the cumulative number of meteoroids larger than 10^{-7} and 10^{-9} kg respectively.
[8] Estimate with http://www.lpl.arizona.edu/tekton/crater_c.html.

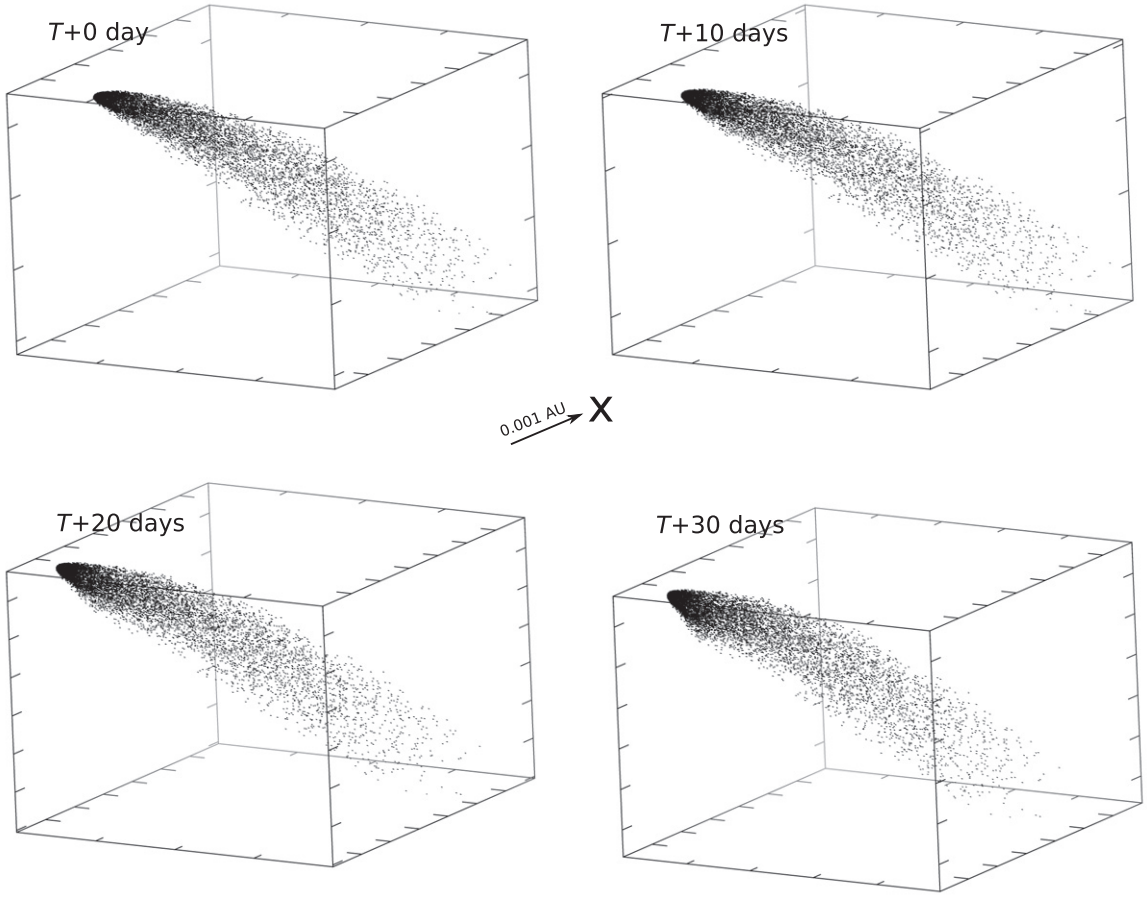

Figure 11. Evolution of the dust tail after the gravitational perturbation of Mars, from $T + 0$ day (encounter) to $T + 30$ days. The graphs are constructed in ecliptic coordinate system, with the X-axis pointing to the vernal point.

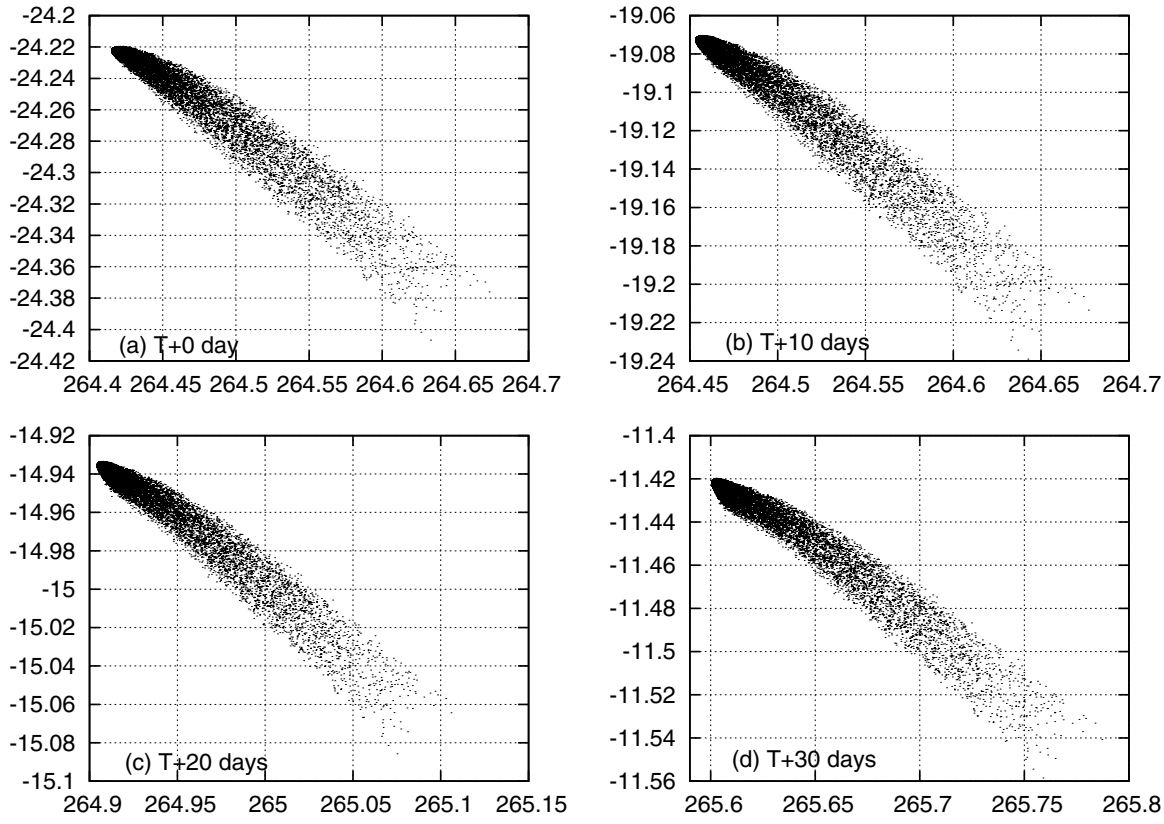

Figure 12. Evolution of the dust tail after the encounter as observed from the Earth.

5.3. Possibility of a Gravitational Disrupted Tail

As one of the closest cometary approaches to a major planet among known objects, we expect the dust tail of C/Siding Spring to be disrupted by the gravitational field of Mars to some degree. To investigate this matter, we integrate a snapshot of the locations of some 12,000 dust particles (generated from previous simulations under the nominal condition) from $T + 0$ to $T + 30$ days (where T is the time of closest approach). The integration is performed with the HNBODY package (Rauch & Hamilton 2002) using the symplectic intergrator, with the barycenter of the Martian system included. The result is shown in Figures 11 and 12. We find that at $T + 20$ days, the apparent size of the "clump" reaches of the order of $0.^{\circ}01$ or $30''$ as seen on Earth, which may be detectable by ground-based telescopes.

6. CONCLUSION

We reported on the the observations and modeling works of C/Siding Spring, a dynamically new comet that will make a close approach to Mars on 2014 October 19. By fitting the observations with syndyne simulations, we found that the tail of C/Siding Spring was dominated by larger particles at the time of its observation. Synchrone simulation suggested that the particles dominating the optical tail were released by the comet as early as late 2012, when the comet was more than ~7 AU from the Sun. We then developed a semi-analytic model to simulate the cometary dust activity. The modeling result suggested a modest ejection velocity of C/Siding Spring that is comparable to a few other comets, including P/Churyumov–Gerasimenko, the target of the *Rosetta* mission.

The same model was then used to study the meteoroid influence on Mars during the encounter, fed with the constraints found in the previous steps. We found that the planet will miss the dust cone by some 20 Martian radii (67,800 km) under the nominal situation. Although the planet may be engulfed by the cometary dust tail if we made an educated guess about the uncertainties and pushed the parameters to the most extreme cases, the simulation suggested that the meteoroids that reach the vicinity of Mars are dominated by non-spacecraft-threatening meteoroids, and the meteoric influx is not significantly higher than the sporadic background influx; the duration of the event is of the order of 1 hr. From our simulation, it seems that an intense and enduring meteoroid bombardment of Mars and its vicinity is unlikely during the flyby of C/Siding Spring.

We also study the potential gravitational disruption of the cometary dust tail. A simple numerical integration suggested that the dust "clump" created by the gravitational drag would be of the order of tens of arcsecs at $T + 20$ days as seen from Earth, which may be detectable by ground-based facilities.

At the time of the writing, C/Siding Spring is about 4 AU from the Sun. As the comet travels into the inner solar system and enters the water–ice sublimation line, its progress could evolve dramatically. We encourage observers to closely monitor C/Siding Spring as it helps on creating a full picture of this unprecedented cosmic event.

Note added: at the reviewing stage of this paper, J. Vaubaillon et al. also reported their modeling result of the same event (see Vaubaillon et al. 2014). Our initial check using their input values suggested an order-of-magnitude agreement between the two results, which indicated that the difference between the two results is primary due to input parameters.

We thank an anonymous referee for comments. We are indebted to the Jade Scope team led by Angus Lau, who kindly allowed us to use their facility in Australia and did a lot of work executing the observations and dealing with instrumental issues. We also thank Xing Gao of the Xingming Observatory for the C/ISON data and his long-term support with the Xingming facilities. We thank Peter Brown, Matthew Knight, Jian-Yang Li, and Paul Wiegert for their help and discussions. Q.-Z. thanks Peter Brown for his support and Summer Xia Han for encouraging him to overcome his laziness and urging him to complete the manuscript.

We also thank the following "Cometas Obs" observers for their $Af\rho$ measurements: José Ramón Vidal Blanco, Josep María Bosch, Montse Campas, García Cuesta, José Francisco Hernández, Gustavo Muler, Ramon Naves, and the unspecified observers at Moorook and Siding Spring Observatories.

REFERENCES

Agarwal, J., Müller, M., Reach, W. T., et al. 2010, Icar, 207, 992
A'Hearn, M. F., Belton, M. J. S., Collins, S. M., et al. 2008, EP&S, 60, 61
A'Hearn, M. F., Schleicher, D. G., Millis, R. L., Feldman, P. D., & Thompson, D. T. 1984, AJ, 89, 579
Brown, P., & Jones, J. 1998, Icar, 133, 36
Ceplecha, Z., Borovička, J., Elford, W. G., et al. 1998, SSRv, 84, 327
Crifo, J. F. 1995, ApJ, 445, 470
Domokos, A., Bell, J. F., Brown, P., et al. 2007, Icar, 191, 141
Finson, M. J., & Probstein, R. F. 1968, ApJ, 154, 327
Ishiguro, M. 2008, Icar, 193, 96
Ishiguro, M., Sarugaku, Y., Ueno, M., et al. 2007, Icar, 189, 169
Knight, M. M., & Walsh, K. J. 2013, ApJL, 776, L5
Le Feuvre, M., & Wieczorek, M. A. 2011, Icar, 214, 1
Li, J.-Y., Kelley, M. S. P., Knight, M. M., et al. 2013, ApJL, 779, L3
Ma, Y., Williams, I. P., & Chen, W. 2002, MNRAS, 337, 1081
McNamara, H., Jones, J., Kauffman, B., et al. 2004, EM&P, 95, 123
McNaught, R. H., Sato, H., & Williams, G. V. 2013, CBET, 3368, 1
Moorhead, A. V., Wiegert, P. A., & Cooke, W. J. 2014, Icar, 231, 13
Rauch, K. P., & Hamilton, D. P. 2002, BAAS, 34, 938
Reach, W. T., Sykes, M. V., Lien, D., & Davies, J. K. 2000, Icar, 148, 80
Ryabova, G. O. 2013, SoSyR, 47, 219
Stokes, G. H., Yeomans, D. K., Bottke, W. F., et al. 2003, in Report of the Near-Earth Object Science Definition Team, 21 (http://neo.jpl.nasa.gov/neo/neoreport030825.pdf)
Strom, R. G., Malhotra, R., Ito, T., Yoshida, F., & Kring, D. A. 2005, Sci, 309, 1847
Vaubaillon, J., Colas, F., & Jorda, L. 2005, A&A, 439, 751
Vaubaillon, J., Maquet, L., & Soja, R. 2014, MNRAS, 439, 3294
Whipple, F. L. 1951, ApJ, 113, 464
Williams, I. P., & Fox, K. 1983, in Asteroids, Comets, and Meteors, ed. C.-I. Lagerkvist & H. Rickman (Uppsala, Sweden: Astronomiska Observatoriet), 399
Ye, Q., & Wiegert, P. A. 2014, MNRAS, 437, 3283
Ye, Q., Wiegert, P. A., Brown, P. G., Campbell-Brown, M. D., & Weryk, R. J. 2014, MNRAS, 437, 3812
Yeomans, D. K., & Chamberlin, A. B. 2013, AcAau, 90, 3
Zacharias, N., Monet, D. G., Levine, S. E., et al. 2004, BAAS, 36, 1418